VIP Nanocrystals

DOI: 10.1002/anie.201302867

Compositionally Tunable Photoluminescence Emission in $Cu_2ZnSn(S_{1-x}Se_x)_4$ Nanocrystals**

*Ajay Singh, Shalini Singh, Sergiu Levcenko, Thomas Unold, Fathima Laffir, and Kevin M. Ryan**

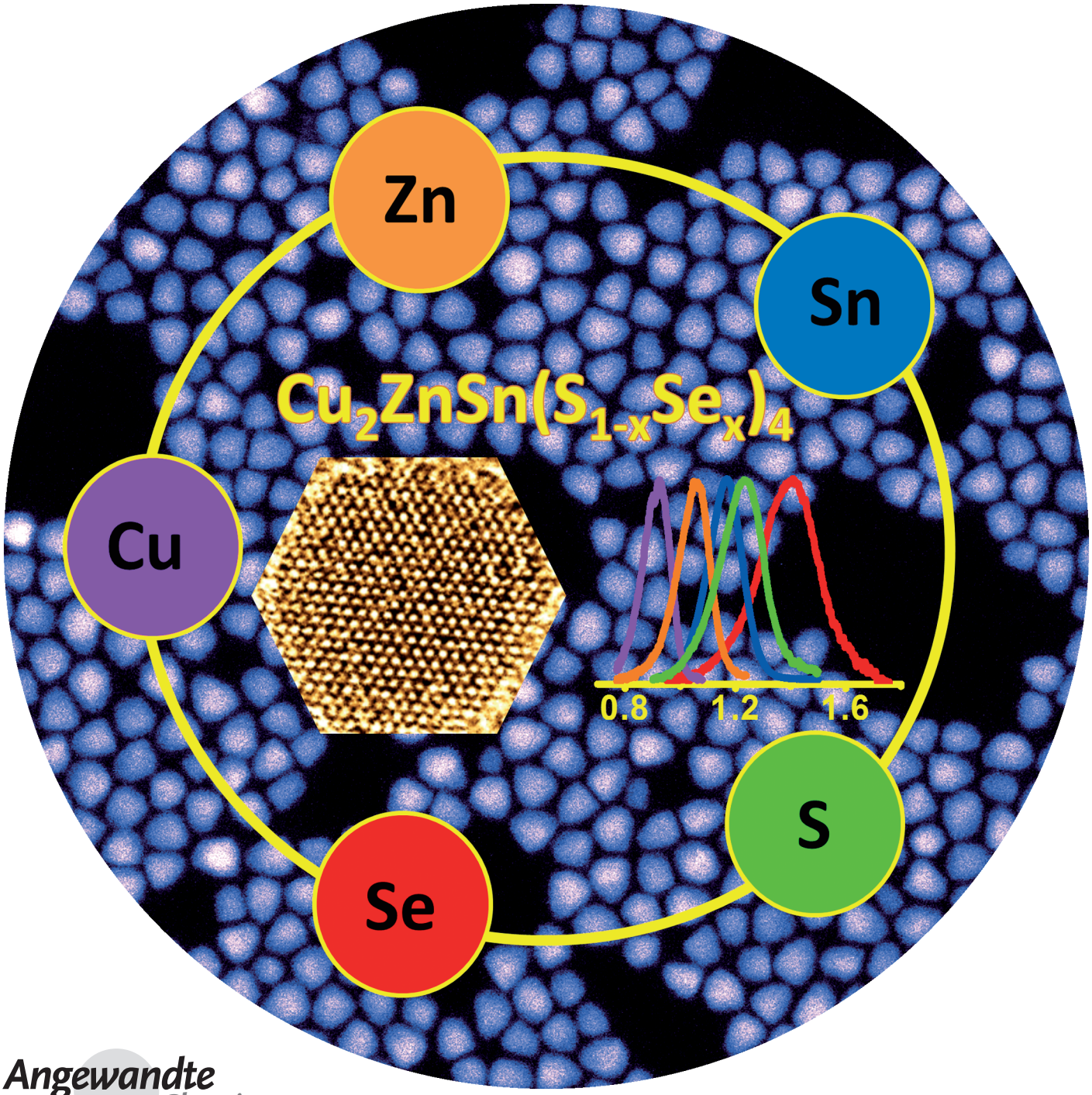

Multicomponent copper chalcogenide-based compounds, namely Cu_2ZnSnS_4 (CZTS), $Cu_2ZnSnSe_4$ (CZTSe), $Cu_2ZnSn(S_{1-x}Se_x)_4$ (CZTSSe), and $Cu_2Zn(Sn_{1-x}Ge_x)(S_{1-y}Se_y)_4$ (CZTGSSe), which were obtained by colloidal nanocrystal syntheses, have recently attracted a great deal of attention because of their low toxicity, earth abundance of the constituent elements, and suitable band-gap for solar energy conversion.[1,2] Synthesizing these materials in nanocrystal form has advantages, as it allows for wet-chemical processing enabling thin-film formation at a fraction of the costs of vacuum-based processes.[1a–d] The best photovoltaic (PV) efficiencies (8.4%) have been achieved when the nanocrystal films are subsequently annealed or selenized to recrystallize into conventional kesterite layers.[1b] The retention of the (I_2-II-IV-VI_4) semiconductors in nanocrystal form is also of significant interest as potential replacements for cadmium-based quantum dots in biological tagging, sensitizers for dye solar cells or as components for nanoelectronic devices.[3] While the Bohr radius is typically too small for quantum confinement effects to manifest,[4] the ability to tune the band-gap by control of stoichiometry allows for more versatile tuning of optical properties.[5] Despite the high optical absorption coefficients ($>10^4\,cm^{-1}$ above the band-gap) observed in the bulk,[6] the copper chalcogenides in colloidal nanocrystal form do not show a pronounced absorbance edge thereby presenting a limitation to reliable determination of the band-gap.[1,2,7] Tauc plots require defined inflections and different reports have shown band-gaps that significantly vary for similar compositions of CZTSSe nanocrystals.[2c–f] Herein, we present the first low-temperature photoluminescence (PL) study on earth-abundant copper chalcogenide (CZTSSe) nanocrystals. Synthetic control of the sulfur/selenium ratio results in a defined shift in the PL emission exactly consistent with the stoichiometric composition. Systematic variation of the sulfur/selenium ratio allows the band-gap to be tuned from 1.4 to 0.9 eV. The tunable PL emission in earth abundant quaternary chalcogenides greatly expands their potential application in both discrete nanocrystal (Q-dot) applications and in thin-film PV devices where a defined and controllable band-gap is required.[1a–c,3,5]

The $Cu_2ZnSn(S_{1-x}Se_x)_4$ nanocrystals are synthesized in wurtzite form with selenium incorporation achieved by a modification of our previous CZTS nanocrystal synthesis.[2a] Figure 1 shows the normalized PL spectra of the wurtzite (W-$Cu_2ZnSn(S_{1-x}Se_x)_4$ nanocrystals at 20 K (see Figure S1 in the Supporting Information for optical absorption). The $Cu_2ZnSn(S_{1-x}Se_x)_4$ PL spectra show one broad emission band which is gradually tuned from 1.4 eV for $x=0$ to 0.9 eV for $x=0.8$. The dip at about 0.9 eV for $x=0.8$ is due to the absorption of water vapor. Assuming that the observed PL bands originate from near band-edge emission of W-$Cu_2ZnSn(S_{1-x}Se_x)_4$ nanocrystals, the variation of the band-gap within experimental error can be well-approximated using the empirical equation $E_g(x)=1.37–0.54\,x$, from which a value of about $0.83+/-0.02$ eV for the W-CZTSe band-gap can be estimated (see E1 and Figure S2 in the Supporting Information). The W-$Cu_2ZnSn(S_{1-x}Se_x)_4$ nanocrystals therefore yield band-gaps that are chemically tunable within a range of ΔE (ca. 0.6 eV) simply by altering the chalcogen ratio.

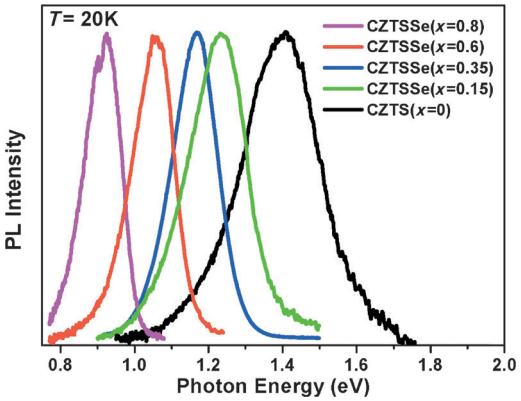

Figure 1. Low-temperature photoluminescence (PL) emission of $Cu_2ZnSn(S_{1-x}Se_x)_4$ nanocrystals with varying values of x.

The PL emission trends match well with results for similar compositions generated using hydrazine-based and vacuum-based deposition routes in well-studied thin-film systems.[8a] The pure CZTS signal (Figure S3) is weak in comparison to the selenized analogs suggesting the inclusion of Se has a greater effect on minimizing the surface or other recombination events. This is similar to behavior in cadmium chalcogenides where the metal selenides show an enhanced and narrow photoemission in comparison to the sulfides in the absence of a defined capping semiconductor shell.[8b,c] The excellent fit to the expected band-gap values as a function of the composition as shown in this PL analysis offers a very reliable verification of optoelectronic properties.

Obtaining the correct compositions in a homogeneous alloy is not trivial considering that five different elemental precursors of varying reactivities are incorporated in a wet-chemical system.[9] The $Cu_2ZnSn(S_{1-x}Se_x)_4$ nanocrystals were obtained by using a hot injection colloidal synthesis method adapted from our previous report (see the full experimental

[*] Dr. A. Singh,[+] S. Singh, Dr. F. Laffir, Dr. K. M. Ryan
Department of Chemical and Environmental Sciences Materials and Surface Science Institute (MSSI), University of Limerick (Ireland)
E-mail: kevin.m.ryan@ul.ie
Dr. A. Singh,[+] Dr. K. M. Ryan
The SFI-Strategic Research Cluster in Solar Energy Research
University of Limerick (Ireland)
Dr. S. Levcenko, Dr. T. Unold
Helmholtz-Zentrum Berlin für Materialien und Energie
Hahn-Meitner-Platz 1, Berlin (Germany)
[+] Current address:
The Molecular Foundry
Lawrence Berkeley National Laboratory (USA)

[**] This work was supported by the Science Foundation Ireland (SFI) through the Principal Investigator program. Contract number 11-PI-48 and the Solar Energy Conversion Strategic Research Cluster (grant number 07/SRC/B1160). A.S. thanks the SFI STTF and HZB for the support. S.L. thanks the Humboldt foundation for support.
Supporting information for this article is available on the WWW under http://dx.doi.org/10.1002/anie.201302867.

details in the Supporting Information).[2a,9c,d] The selection of a suitable selenium precursor, diphenyl diselenide (DPSe) in this case, with similar properties (reactivity, solubility, and boiling point) to the sulfur precursor is critical to allow accurate control of the chalcogen ratios (see the Supporting Information for further discussion on precursor selection). The 1-dodecanethiol (1-DDT) concentration is fixed and is in excess as it acts as a capping ligand in addition to the sulfur source.[1g,2a] The selenium composition of the combined chalcogen precursor solution strongly correlates to the final stoichiometry obtained. Figure 2 shows transmission electron

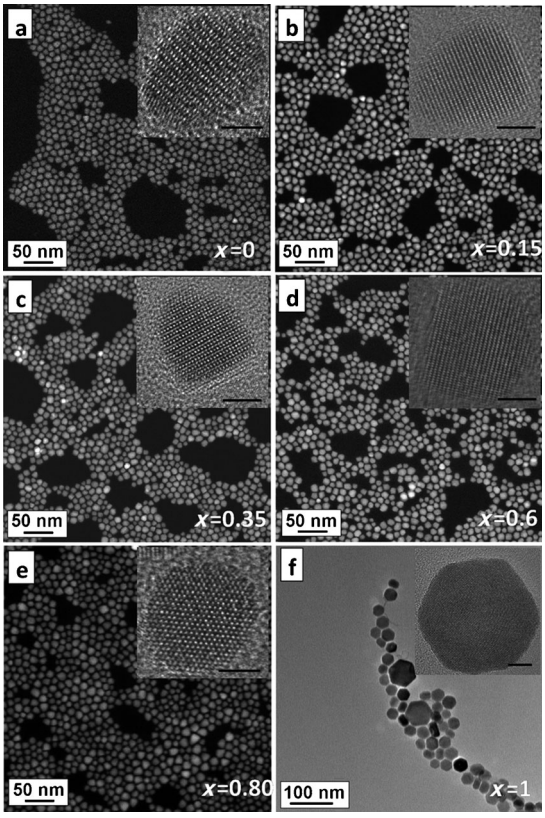

Figure 2. a–f) Dark-field STEM (DF-STEM) and TEM images of pseudo-spherical $Cu_2ZnSn(S_{1-x}Se_x)_4$ nanocrystals with a) x–0, b) x–0.15, c) x–0.35, d) x–0.6, e) x–0.8, and f) x–1. The insets show the HRTEM image of the single-nanocrystals (the scale bars are 5 nm).

microscopy images of $Cu_2ZnSn(S_{1-x}Se_x)_4$ nanocrystals where x varies from 0 (CZTS) to 1 (CZTSe) in defined increments. The particles containing sulfur ($x = 0$–0.8) are pseudo-spherical in shape and of low polydispersity 11 ± 2 nm as seen in low-resolution angular dark-field scanning transition electron microscopy (DF-STEM; Figure 2 a–e). The inset high-resolution TEM images show that nanocrystals are highly crystalline with continuous lattice fringes throughout. CZTSe nanocrystals (Figure 2 f) form with a different crystal habit with a hexagonal disc shape preferred. This is due to the absence of the 1-DDT in its capping ligand role which has been shown previously to passivate growth facets other than the (001) in the quaternary chalcogenide system.[2a,9c] Oleic acid was used as a replacement ligand for 1-DDT and while it does not carry out a similar passivating role, it was critical to retaining the wurtzite phase for this composition, with kesterite CZTSe nanocrystals occurring in its absence (for details see the Supporting Information). All particles form in the metastable wurtzite structure with typical electron diffraction (SAED) Figure S4 showing characteristic (101), (002), and (102) planes. The elemental composition of $Cu_2ZnSn(S_{1-x}Se_x)_4$ nanocrystals was further analyzed by using energy dispersive X-ray spectroscopy. All samples have similar Cu:Zn:Sn ratio (2:1:1) with Se content ranging from $x = 0$–1 in excellent agreement with the amount of DPSe added (see Table S1).

The crystal structure of the $Cu_2ZnSn(S_{1-x}Se_x)_4$ nanocrystal was further characterized by X-ray diffraction (XRD; Figure 3 a). The major reflections can be indexed to (100), (002),

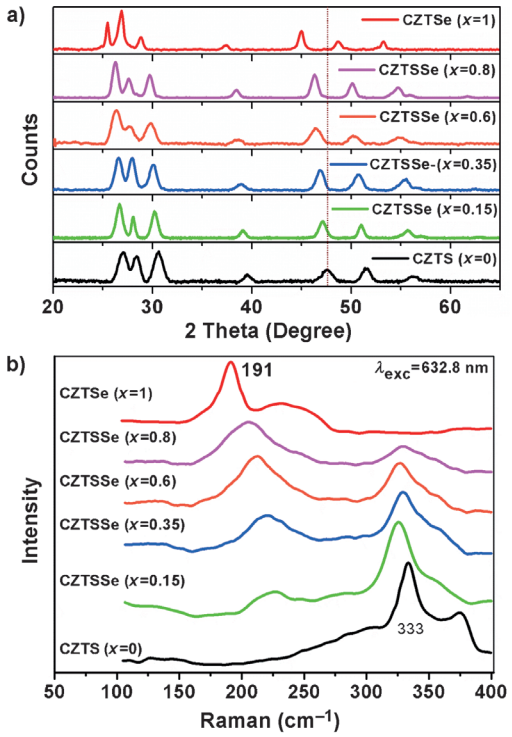

Figure 3. a) Powder XRD pattern of W-$Cu_2ZnSn(S_{1-x}Se_x)_4$ nanocrystals with varying values of x. b) Room-temperature Raman spectra of $Cu_2ZnSn(S_{1-x}Se_x)_4$ nanocrystals with varying values of x.

(101), (102), (110), (103), and (112) reflections of the hexagonal structure. Furthermore, the XRD pattern for $x =$ 0 and 1 matches well with the simulated wurtzite crystal structure (see Figure S5 in the Supporting Information). The systematic shift in peak position toward lower angles as x increases correlates with the replacement of larger Se atoms with smaller S atoms. (This is highlighted in Figure S6a for the (110) reflection.) The lattice spacing for the (002) planes were calculated and plotted as a function of x (see Figure S6b in the Supporting Information) giving a linear behavior (Vegard's law) with increasing Se content which confirms that the obtained nanocrystal are homogenously alloyed rather than a mixture of CZTS and CZTSe. As XRD may be insufficient

in identifying potential binary (ZnS, ZnSe) and ternary (Cu_3SnS_4, Cu_2SnSe_3) impurities because of similar PXRD pattern to wurtzite CZTSSe, further characterization with Raman was performed to confirm the presence of a single phase. Figure 3b shows the representative Raman spectra of the W-$Cu_2ZnSn(S_{1-x}Se_x)_4$ nanocrystals. The presence of single peaks at 191 cm^{-1}, 333 cm^{-1} for $x=1$ (CZTSe) and $x=0$ (CZTS), respectively, confirms the formation quaternary nanocrystals, and clearly show that there is no presence of ZnSe and ZnS which has a strong Raman peak at 251 and 351 cm^{-1}.[10a,b] For compositions from $x=0.15$ to 0.8, the intensive Raman modes exhibit a two-mode behavior. The wurtzite CZTSe-like mode[2f] strongly shifts from 191 cm^{-1} for $x=1$ to 225 cm^{-1} for $x=0.15$, while the W-CZTS-like mode[2a] barely shifts from 333 cm^{-1} for $x=0$ to 329 cm^{-1} for $x=0.8$. In fact, a similar two-mode behavior was found previously in $Cu_2ZnSn(S_{1-x}Se_x)_4$ nanocrystals.[10c,e] Recently, Khare et al. have calculated phonon density of states (DOS) for kesterite CZTSSe alloys and interpreted a CZTSe-like mode with vibrations of S, Se, and cation atoms, while only Sn and S atom vibrations were found to be responsible for CZTS-like mode.[10f] Therefore the chalcogen ratio has less effect on the CZTS mode.[10e] Assuming that the calculated DOS for kesterite $Cu_2ZnSn(S_{1-x}Se_x)_4$ alloys might be similar to that of W-$Cu_2ZnSn(S_{1-x}Se_x)_4$, our experimental findings on the intensive $Cu_2ZnSn(S_{1-x}Se_x)_4$ modes can be similarly rationalized. However, a theoretical calculation of W-$Cu_2ZnSn(S_{1-x}Se_x)_4$ would need to be done to fully clarify this assumption.

The chemical states of the constituent elements of the as-synthesized $Cu_2ZnSn(S_{1-x}Se_x)_4$ nanocrystal ($x=0.15$) were confirmed using X-ray photoelectron spectroscopy (XPS). The survey spectrum of the as-synthesized $Cu_2ZnSn(S_{1-x}Se_x)_4$ nanocrystal (see Figure S7) shows the presence of Cu, Zn, Sn, S, Se, O, and C. High-resolution spectra of individual elements were further acquired to investigate the oxidation states (Figure 4). The S 2p doublet with S $2p_{3/2}$ at 161.7 eV is attributed to metal sulphide.[11,12,13a] The broad peaks at 160 and 166 eV belong to Se 3p. The Se 3d doublet with spin–orbit coupling of 0.9 eV and Se $3d_{5/2}$ at 54.1 eV is characteristic of the selenide state. The Cu spectrum shows a narrow doublet peak that appears at 932.0 eV ($2p_{3/2}$) and 951.8 eV ($2p_{1/2}$) with a standard separation of 19.8 eV confirming the monovalent copper in the nanocrystal.[11] The peaks of Zn 2p appear at binding energies of 1021.7 and 1044.7 eV, with a doublet splitting of 23.0 eV is indicative of Zn^{II}.[13c] Sn^{IV} is confirmed by characteristic peak separation of 8.4 eV of two peaks located at 486.3 and 494.7 eV, respectively.[11,12] Further compositional analysis indicates a decrease in the ratio of S/Se as the selenide concentration is increased. However, the overall ratio of metal/(S+Se) ratio remains constant indicative of Se replacing S. This further confirms the homogenous nature of $Cu_2ZnSn(S_{1-x}Se_x)_4$ nanocrystals.

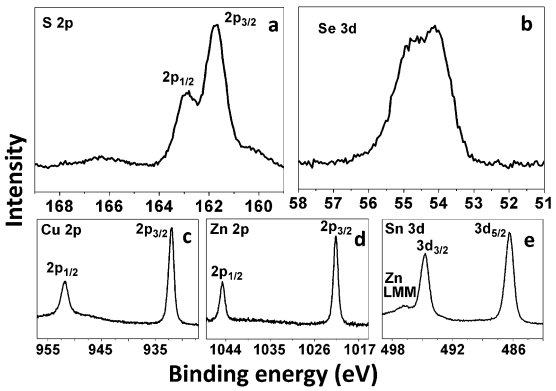

Figure 4. High-resolution XPS spectrum of the $Cu_2ZnSn(S_{1-x}Se_x)_4$ nanocrystal for $x=0.15$.

In summary, we have shown that tunable photoemission from quaternary copper chalcogenides can be achieved by varying the chalcogen ratio in the nanocrystals. This is essentially directly controlled by the concentration of the DPSe that is injected to initiate crystal nucleation with all other species constant. The nanocrystals form in the wurtzite crystal structure as a single $Cu_2ZnSn(S_{1-x}Se_x)_4$ phase of controlled stoichiometry where x can range from 0–1. The band-gap can therefore be systematically tuned within a range of 0.6 eV which has previously been possible only in thin-film systems. These earth-abundant chalcogenides may be of significant interest for photovoltaic and photoemissive applications, as the band-gap and hence photoluminescence emission is significantly tunable with the desired stoichiometry locked in to each crystal.[6]

Received: April 7, 2013
Published online: June 18, 2013

Keywords: chalcogens · colloidal synthesis · inorganic nanostructures · nanocrystals · photoluminescence

[1] a) Q. Guo, G. M. Ford, W.-C. Yang, B. C. Walker, E. A. Stach, H. W. Hillhouse, R. Agrawal, *J. Am. Chem. Soc.* **2010**, *132*, 17384; b) Q. Guo, G. M. Ford, W. C. Yang, C. J. Hages, H. W. Hillhouse, R. Agrawal, *Sol. Energy Mater. Sol. Cells* **2012**, *105*, 132; c) C. Steinhagen, M. G. Panthani, V. Akhavan, B. Goodfellow, B. Koo, B. A. Korgel, *J. Am. Chem. Soc.* **2009**, *131*, 12554; d) G. M. Ford, Q. Guo, R. Agrawal, H. W. Hillhouse, *Chem. Mater.* **2011**, *23*, 2626; e) S. C. Riha, B. A. Parkinson, A. L. Prieto, *J. Am. Chem. Soc.* **2009**, *131*, 12054; f) A. Shavel, J. Arbiol, A. Cabot, *J. Am. Chem. Soc.* **2010**, *132*, 4514; g) M. Ibáñez, R. Zamani, A. LaLonde, D. Cadavid, W. Li, A. Shavel, J. Arbiol, J. R. Morante, S. Gorsse, G. J. Snyder, A. Cabot, *J. Am. Chem. Soc.* **2012**, *134*, 4060; h) M. Ibáñez, D. Cadavid, R. Zamani, N. García-Castelló, V. Izquierdo-Roca, W. Li, A. Fairbrother, J. D. Prades, A. Shavel, J. Arbiol, A. Pérez-Rodríguez, J. R. Morante, A. Cabot, *Chem. Mater.* **2012**, *24*, 562.

[2] a) A. Singh, H. Geaney, F. Lafir, K. M. Ryan, *J. Am. Chem. Soc.* **2012**, *134*, 2910; b) A. Shavel, D. Cadavid, M. Ibáñez, A. Carrete, A. Cabot, *J. Am. Chem. Soc.* **2012**, *134*, 1438; c) S. C. Riha, B. A. Parkinson, A. L. Prieto, *J. Am. Chem. Soc.* **2011**, *133*, 15272; d) Z. Yang, H. Wei, Z. C. Ye, M. Li, Y. J. Su, Y. F. Zhang, *CrystEngComm* **2011**, *13*, 2222; e) M. E. Norako, M. J. Greaney, R. L. Brutchey, *J. Am. Chem. Soc.* **2012**, *134*, 23; f) X. Lin, J. Kavalakkatt, K. Kornhuber, D. Abou-Ras, S. Schorr, M. C. Lux-Steiner, A. Ennaoui, *RSC Adv.* **2012**, *2*, 9894; g) M. Ibáñez, R.

Zamani, W. Li, A. Shavel, J. Arbiol, J. R. Morante, A. Cabot, *Cryst. Growth Des.* **2012**, *12*, 1085.
[3] a) E. Sakai, *J. Phys. Chem. C* **2012**, *116*, 23945; b) Y. Zhao, C. Burda, *Energy Environ. Sci.* **2012**, *5*, 5564; c) Y. Cao, Y. Xiao, J.-Y. Jung, H.-D. Um, S.-W. Jee, H. Mi Choi, J. Ho Bang, J. Ho Lee, *ACS Appl. Mater. Interfaces* **2013**, *5*, 479; d) X. Xin, M. He, W. Han, J. Jung, Z. Lin, *Angew. Chem.* **2011**, *123*, 11943; *Angew. Chem. Int. Ed.* **2011**, *50*, 11739.
[4] C. Persson, *J. Appl. Phys.* **2010**, *107*, 053710.
[5] a) H. Zhong, Z. Bai, B. Zou, *J. Phys. Chem. Lett.* **2012**, *3*, 3167; b) S. E. Habas, H. A. S. Platt, M. F. A. M. van Hest, D. S. Ginley, *Chem. Rev.* **2010**, *110*, 6571.
[6] "Future Directions for Solution-Based Processing of Inorganic Materials": a) M. F. A. M. van Hest, D. S. Ginley in *Solution Pro-cessing of Inorganic Materials* (Ed.: D. B. Mitzi), Wiley-VCH, Hoboken, NJ, **2008**; b) H. Katagiri, *Thin Solid Films* **2005**, *480*, 426.
[7] a) J. J. Wang, D. J. Xue, Y. G. Guo, J. S. Hu, L. J. Wan, *J. Am. Chem. Soc.* **2011**, *133*, 18558; b) L. Shi, C. Pei, Y. Xu, Q. Li, *J. Am. Chem. Soc.* **2011**, *133*, 10328.
[8] a) R. Haight, A. Barkhouse, O. Gunawan, B. Shin, M. Copel, M. Hopstaken, D. B. Mitzi, *Appl. Phys. Lett.* **2011**, *98*, 253502; b) S. Shen, Q. Wang, *Chem. Mater.* **2013**, *25*, 1166; c) Y.-K. Kim, C.-J. Choi, *Tailoring the Morphology and the Optical Properties of Semiconductor Nanocrystals by Alloying, Nanocrystal* (Ed.: Y. Masuda), InTech, **2011**, DOI: 10.5772/16427.
[9] a) D. K. Smith, J. M. Luther, O. E. Semonin, A. J. Nozik, M. C. Beard, *ACS Nano* **2011**, *5*, 183; b) F. J. Fan, Yi-X. Wang, X.-J. Liu, L. Wu, S.-H. Yu, *Adv. Mater.* **2012**, *24*, 6158; c) A. Singh, C. Coughlan, F. Laffir, K. M. Ryan, *ACS Nano* **2012**, *6*, 6977; d) C. Coughlan, A. Singh, K. M. Ryan, *Chem. Mater.* **2013**, *25*, 653.
[10] a) Y. C. Cheng, C. Q. Jin, F. Gao, X. L. Wu, W. Zhong, S. H. Li, P. K. Chu, *J. Appl. Phys.* **2009**, *106*, 123505; b) W. Taylor, *Phys. Lett. A* **1967**, *24*, 556; c) K. L. Ou, J. C. Fan, J. K. Chen, C. C. Huang, L. Y. Chen, J. H. Ho, J. Y. Chang, *J. Mater. Chem.* **2012**, *22*, 14667; d) Y. Cao, C. Wang, B. Li, K. Zhang, X. Xu, J. Hu, X. Chen, *Jpn. J. Appl. Phys.* **2011**, *50*, 125001; e) F.-J. Fan, L. Wu, M. Gong, G. Liu, Y. X. Wang, S.-H. Yu, S. Chen, L. W. Wang, X.-G. Gong, *ACS Nano* **2013**, *7*, 1454; f) A. Khare, B. Himmetoglu, M. Cococcioni, E. S. Aydil, *J. Appl. Phys.* **2012**, *111*, 123704.
[11] NIST-XPS database, version 3.5 (http://srdata.nist.gov/xps/).
[12] J. F. Moulder, W. F. Stickle, P. E. Sobol, K. D. Bomben, *Handbook of X-ray Photoelectron Spectroscopy*, PerkinElmer, Corporation Physical Electronics Division, **1992**.
[13] a) G. Loepp, S. Vollmer, G. Witte, C. Wöll, *Langmuir* **1999**, *15*, 3767; b) S. J. Li, Z. C. Zhao, Q. H. Liu, L. J. Huang, G. Wang, D. C. Pan, H. J. Zhang, X. Q. He, *Inorg. Chem.* **2011**, *50*, 11958; c) Q. Guo, S. J. Kim, M. Kar, W. N. Shafarman, R. W. Birkmire, E. A. Stach, R. Agrawal, H. W. Hillhouse, *Nano Lett.* **2008**, *8*, 2982.

